Tomographic Reconstructions with Physics-Informed Neural Radiance Fields

Robert Jarolim
High Altitude Observatory, NCAR

Frontier Development Lab - 2023

C. Hung[2], H. Lamdouar[3], M. Sanner[4], E. Stevenson[5], J. Veitch-Michaelis[6], I. Bouri[7], A. Malanushenko[1], V. Ruzicka[8], C. Urbina-Ortega[9]

Frontier Development Lab - 2022

B. Tremblay[1], A. Munoz[10], M. Bintsi[11], A. Jungbluth[12], M. Santos[13], A. Vourlidas[14], J. Mason[14], S. Sundaresan[15], C Downs[16], R. Caplan[16]

PUNCH Meeting – 21st June 2024

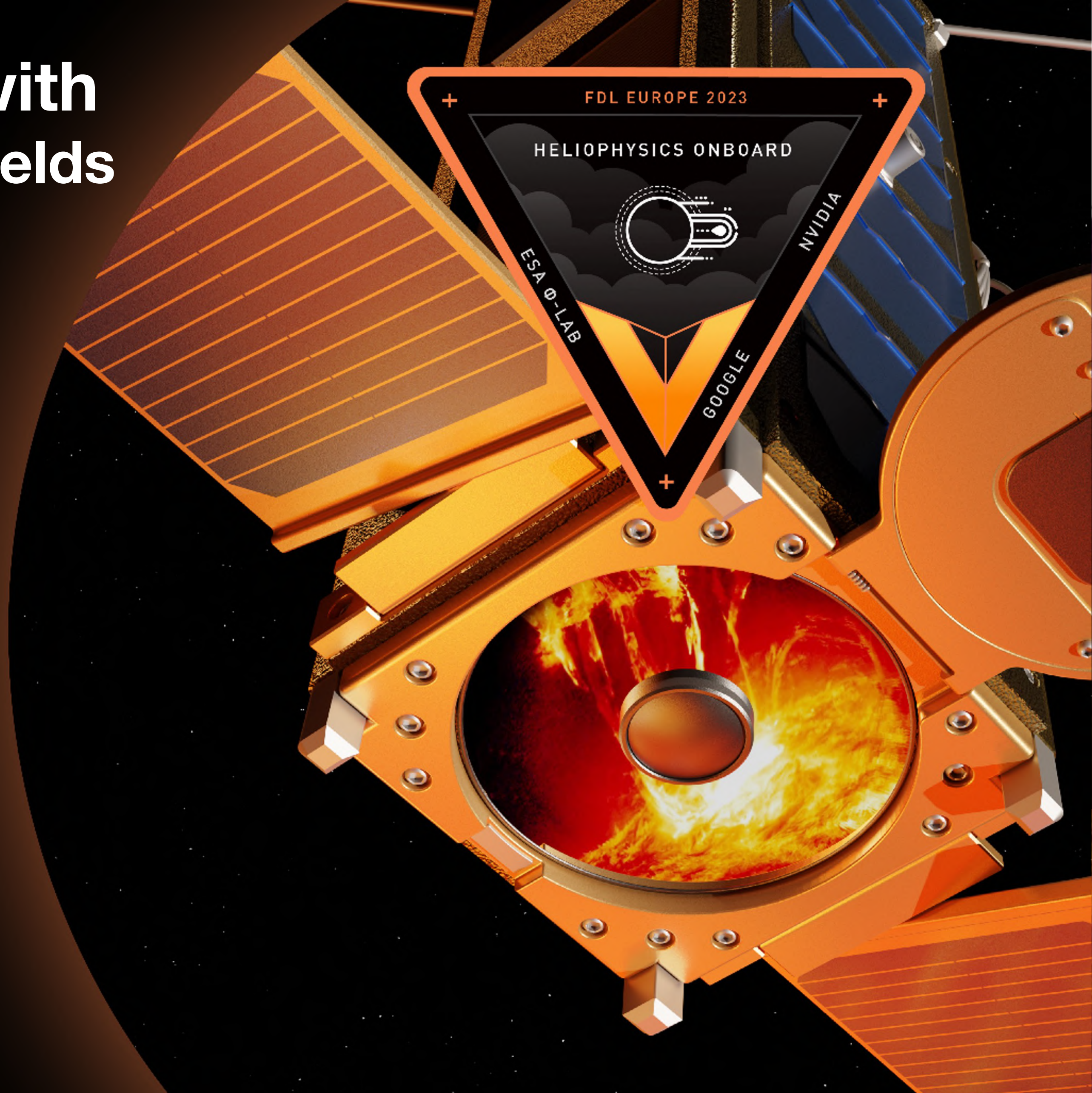

FDLEUROPE.ORG

esa Φ-lab   FDL 2023 EUROPE   Google Cloud   NVIDIA   SCAN AI   Centre for Satellite Data in Environmental Science   PASTEUR iSi   AIRBUS   The Danish Meteorological Institute   D-ORBIT   CATAPULT Satellite Applications   UNIVERSITY OF OXFORD   TRILLIUM EUROPE

Motivation

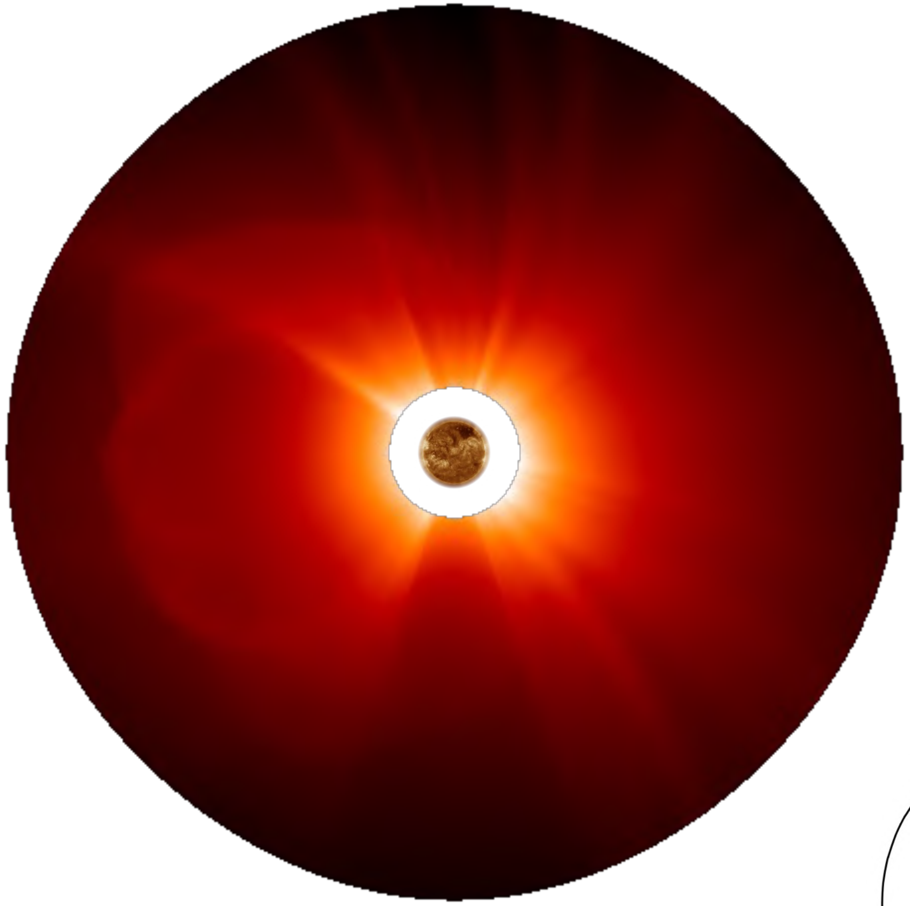

- **Understand the evolution of plasma in the heliosphere**
- Human fitting (e.g., triangulation, CGS reconstr.) is intrinsically limited (e.g., Verbeke et al. 2022)
  - **subjective**
  - **optically-thin** emission
  - Simplified **complexity**

GCS Model – parameter fitting to estimate CME structure (Thernisien, 2011)

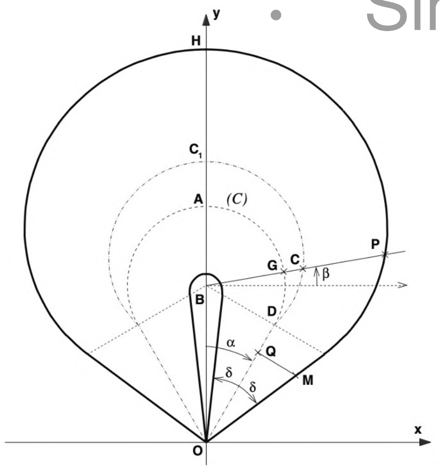

How can we efficiently **combine observations** and **physical models** to determine the **plasma distribution** in the **corona**?

Overview

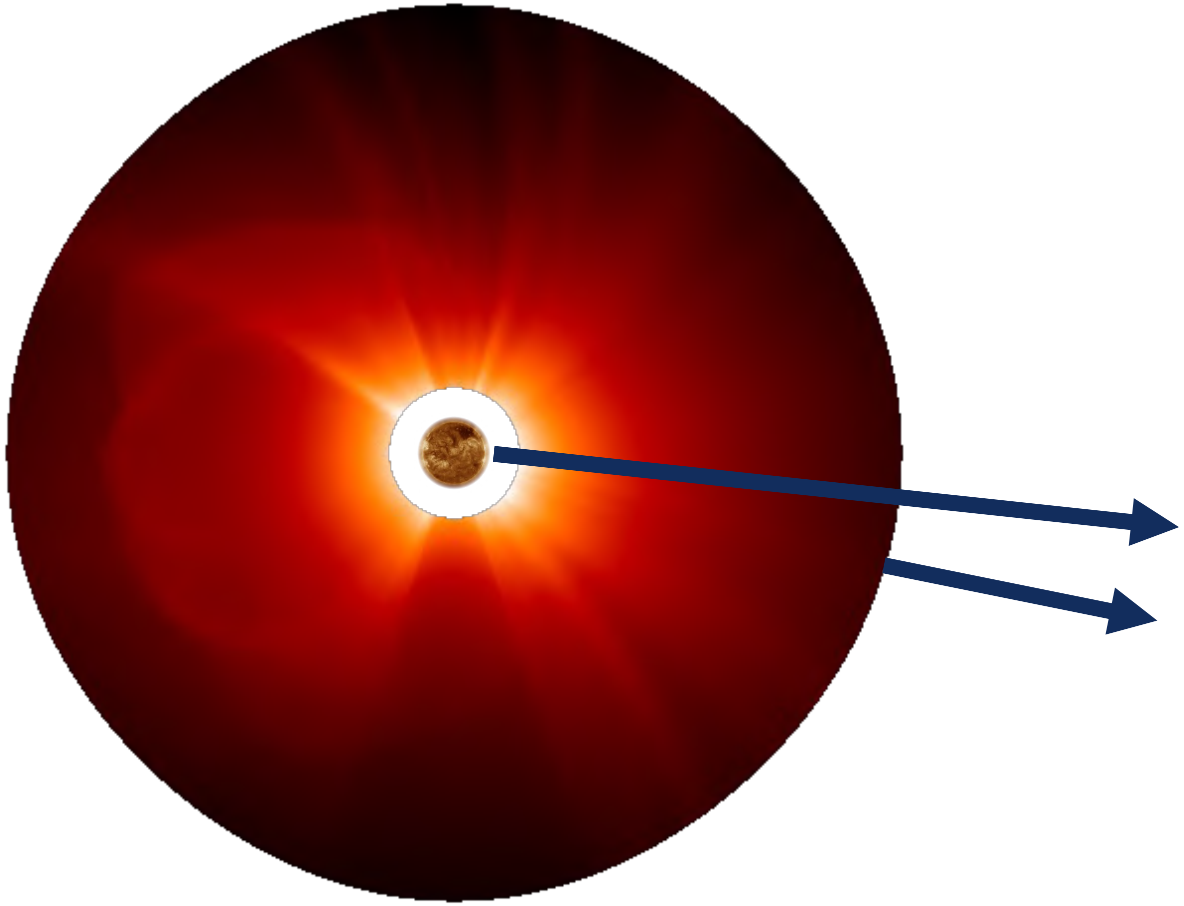

(1) Physics-Informed Neural Networks can integrated observational data and physical models

(2) 4π **EUV corona**

(3) Tomographic reconstruction of **coronal mass ejections**

Physics-Informed machine learning

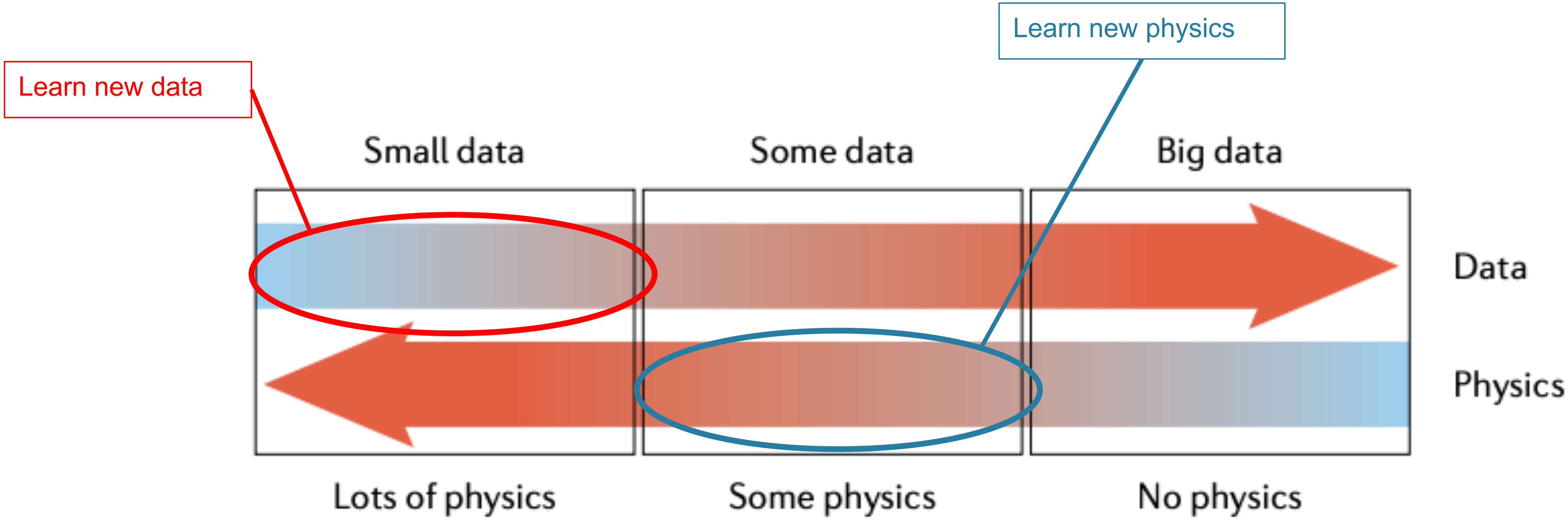

(from Karniadakis et al. 2022)

Physics-Informed Neural Networks (Raissi et al. 2019)

- Small data: known **physics** and **boundary condition**
- **Mesh-free simulation** using Partial Differential Equations (PDEs)
- Advantages over finite differences:
  - More flexibility to account for **noisy data** and **incomplete physical models**
  - Efficient for **high-dimensional problems**
  - **Exact differentials** (independent of mesh)
- Data discovery: **no train/valid/test split**

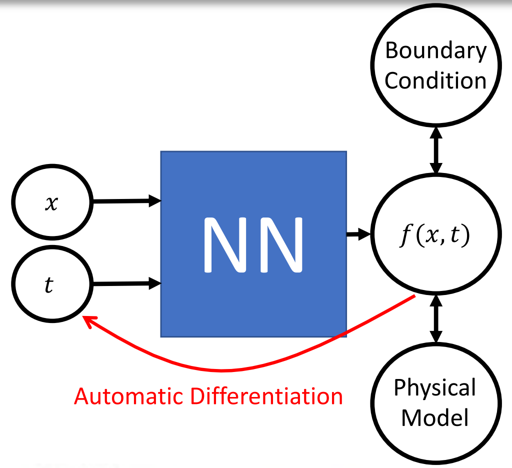

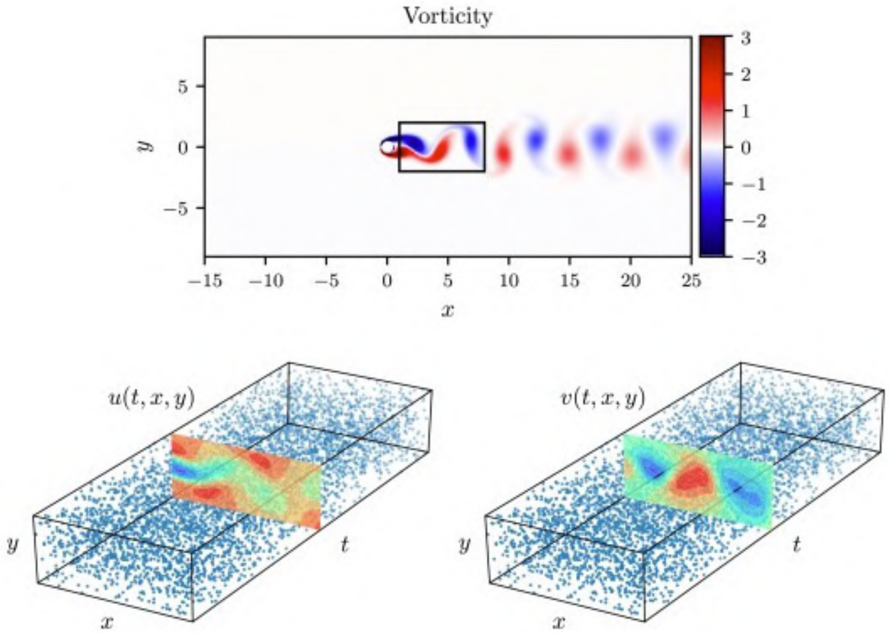

(Solution of Navier-Stokes equation from Raissi et al. 2022)

Tomography of the EUV corona

- SuNeRF – FDL 2023
- Jarolim et al. 2024
  ApJL 961 L31
- Bintsi et al. 2022
  NeurIPS - ML and the Physical Sciences

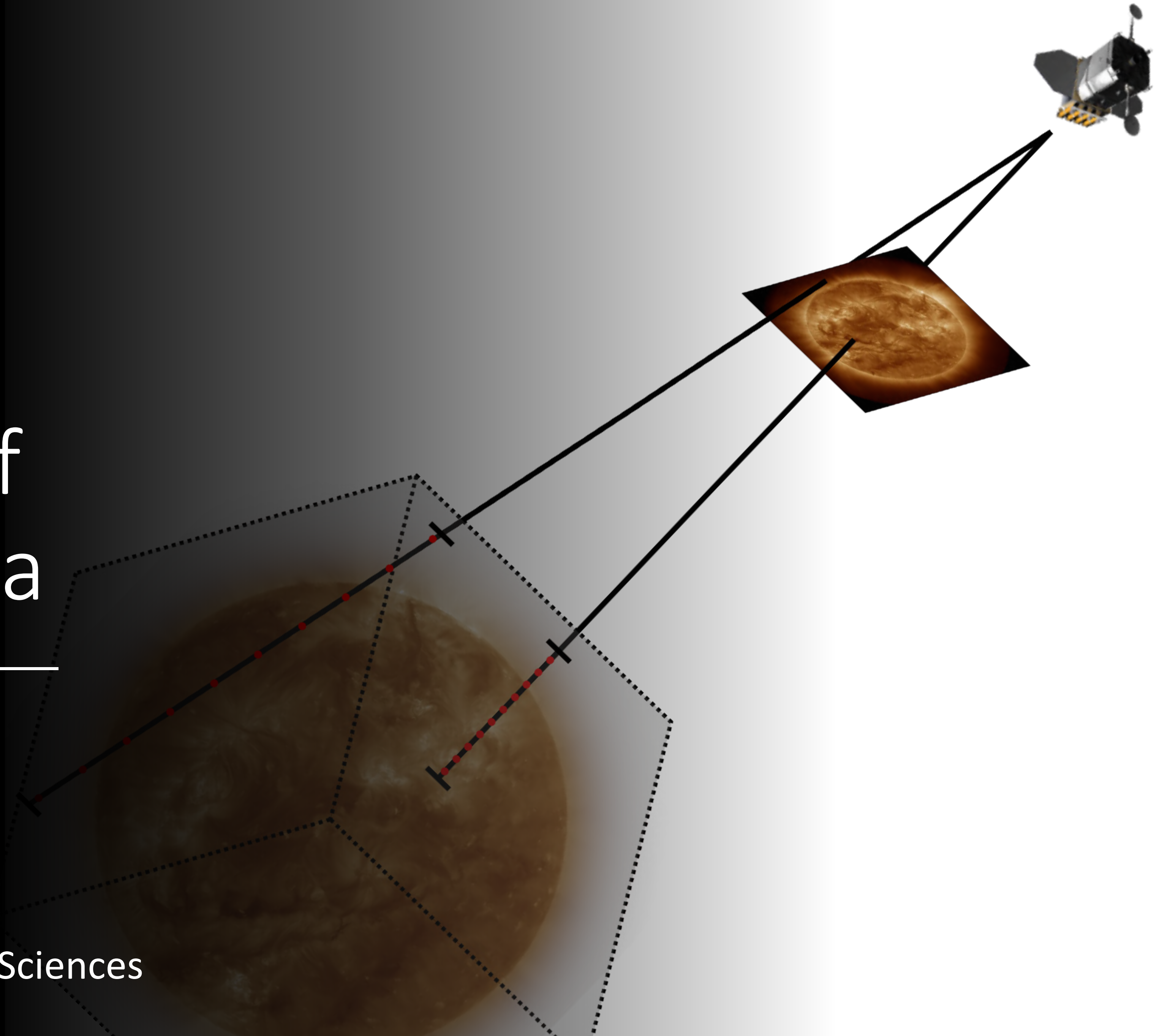

4π EUV corona

- **Limited** amount of **viewpoints** (SDO + STEREO A + B)
  - Optically thin plasma
  - Only ecliptic viewpoints
- Full 3D image enables
  - advanced studies of solar **activity**
  - **Forecasting**
  - connection to other **stars**
- How can we observe the Sun from any perspective?

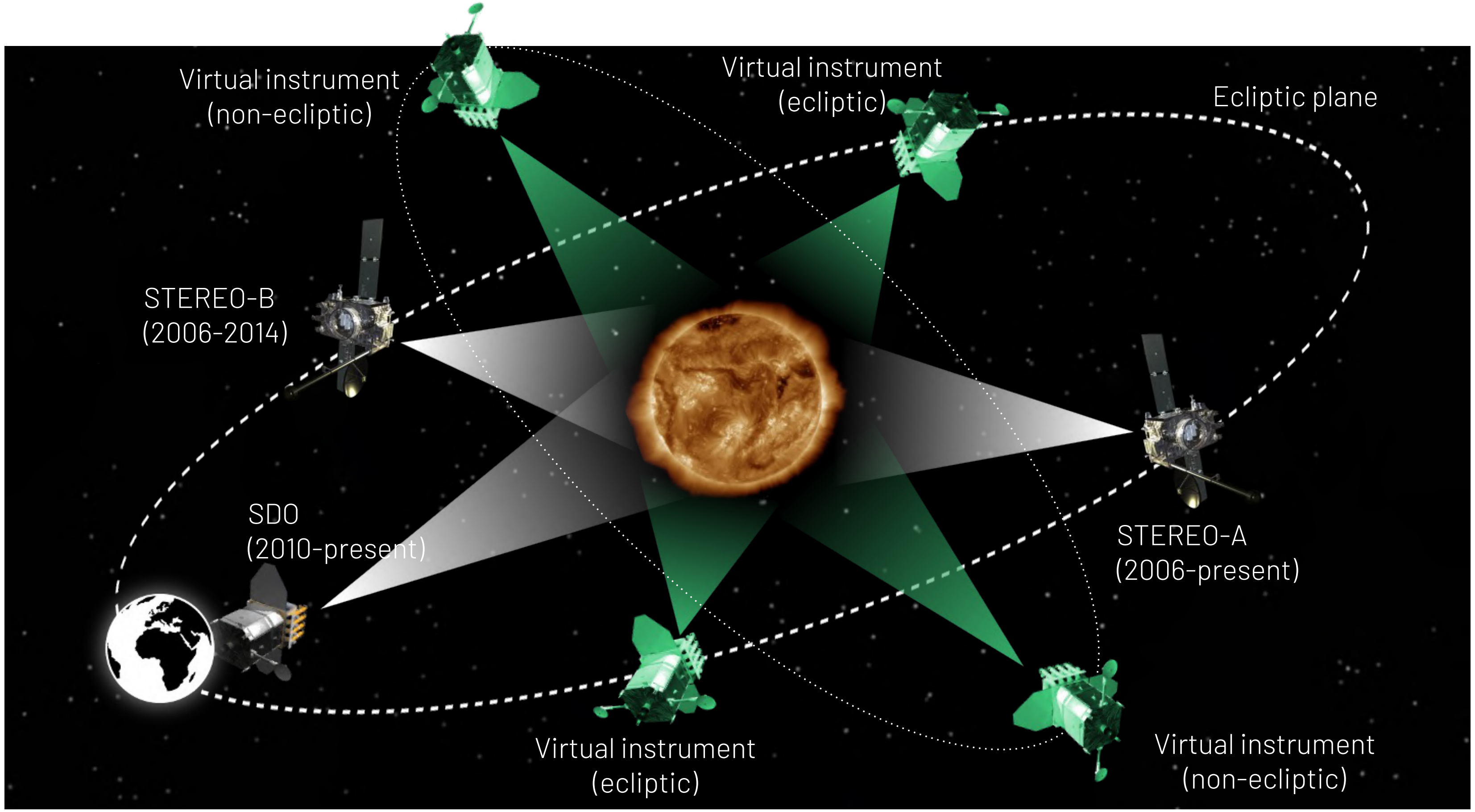

Method: SuNeRF

Sun Neural Radiance Fields:

1. Inputs: sampling along ray (x, y, z)
2. Forward pass
3. Outputs:
   -Emission coefficient
   -Absorption coefficient
4. Integrate pixel intensity along ray
5. Optimization: match observations

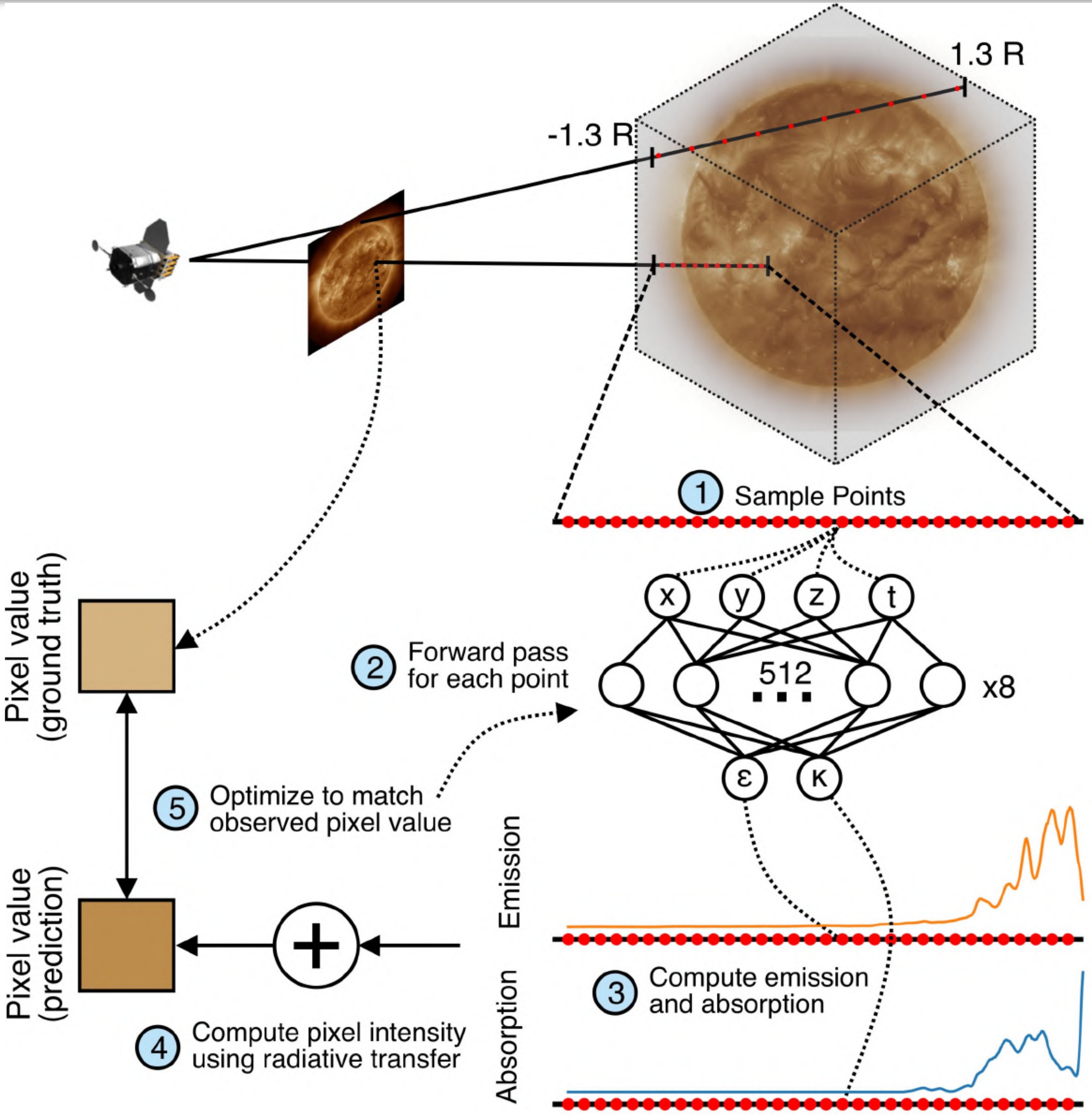

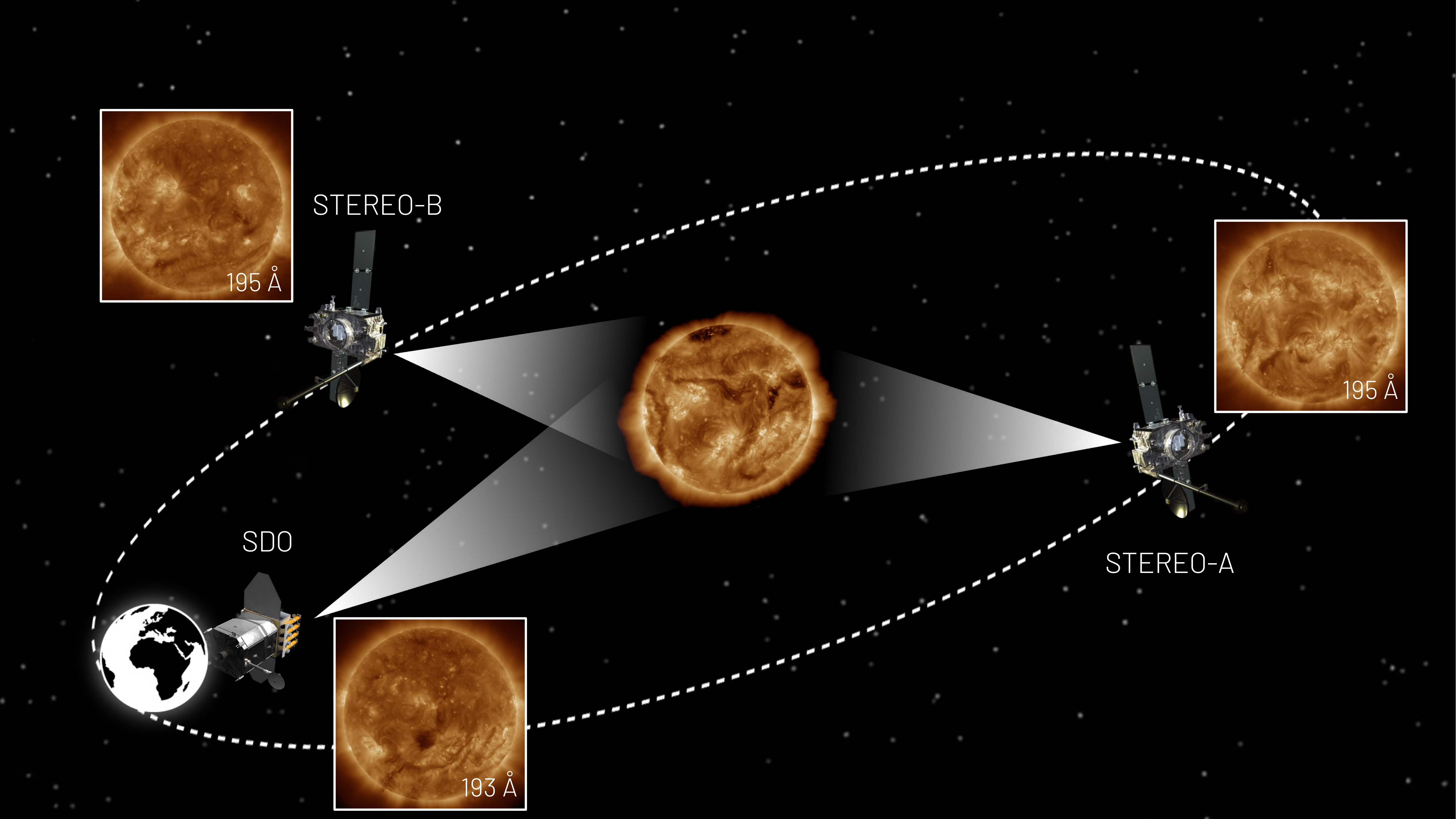

STEREO-B
195 Å
195 Å
STEREO-A
SDO
193 Å

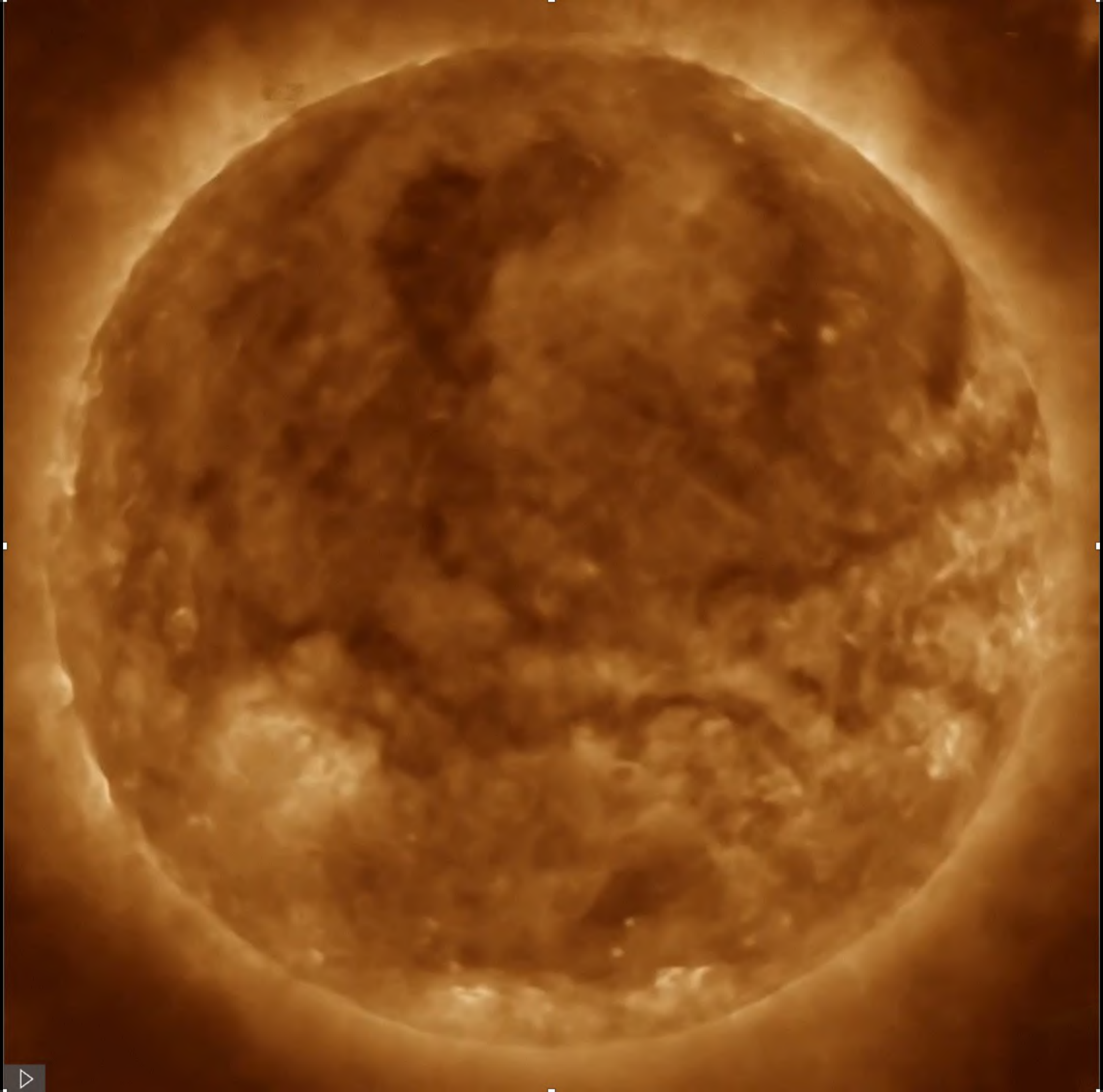

Tomography of Coronal Mass Ejections

- SuNeRF-CME – FDL 2024
- in prep.

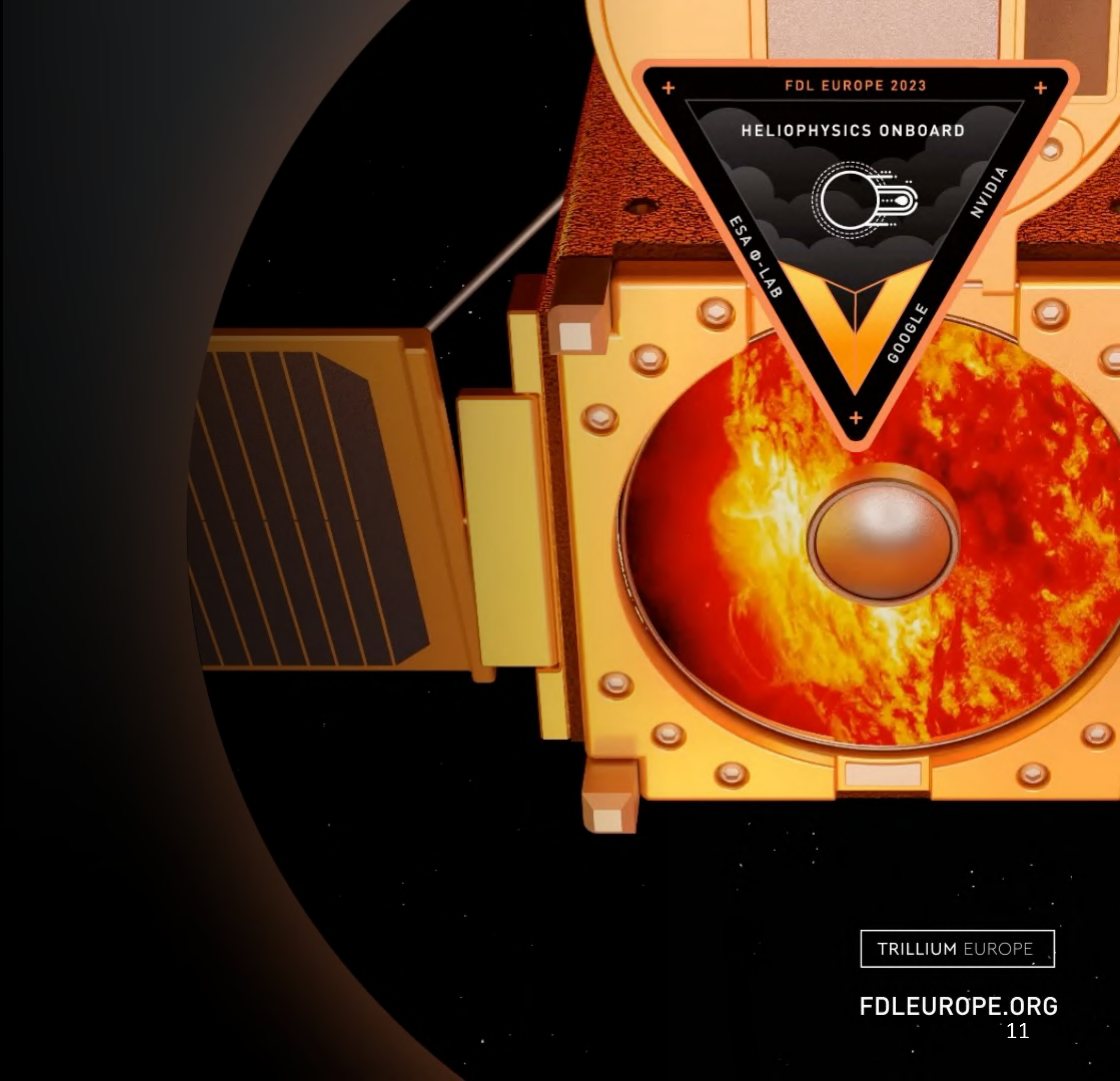

TRILLIUM EUROPE

FDLEUROPE.ORG

Observing capabilities – Coronal Mass Ejections (CMEs)

- CMEs cause the most **severe space weather** effects
- **Optically-thin plasma** limits success of triangulation
- **Direction, Velocity, Mass**

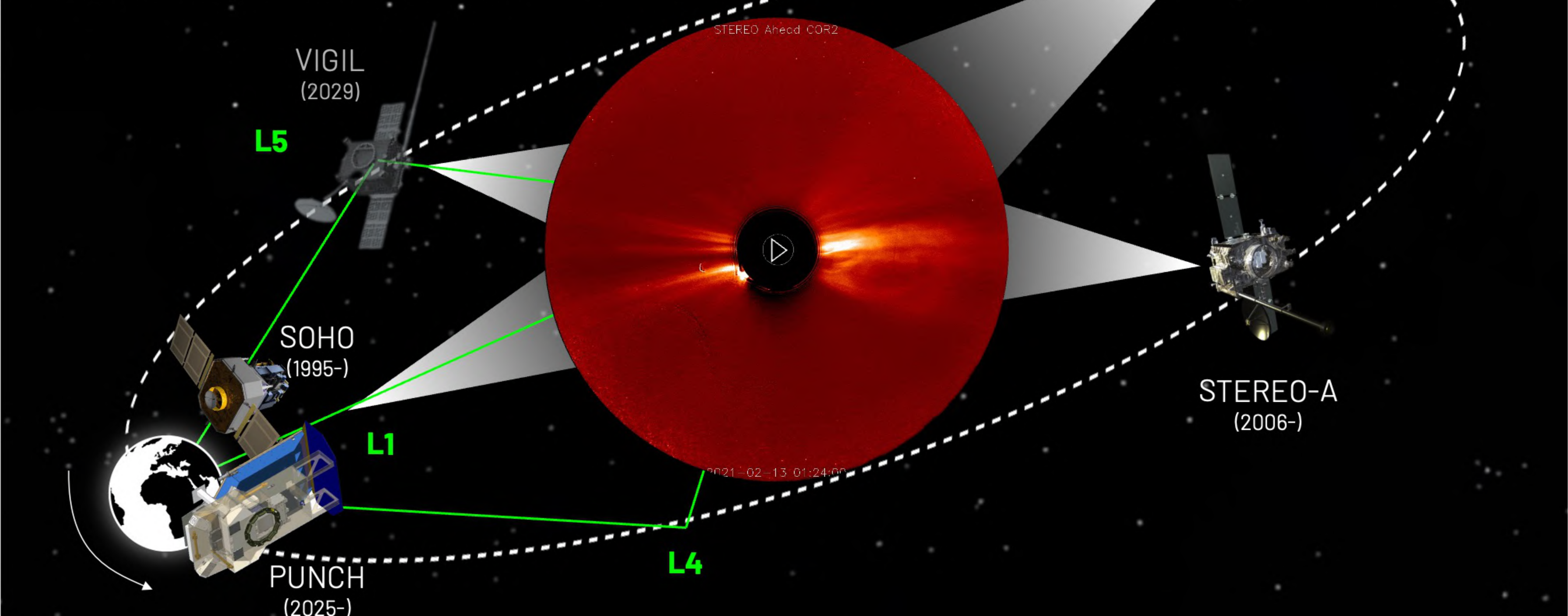

CME Dataset

- Validation with synthetic PUNCH observations (Credits: A. Malanushenko)
  - GAMERA simulation – **0.1 AU to 100 $R_\odot$**
  - Ground truth reference – **electron density**
  - Idealized (no noise, artifacts, background stars)
  - CME in ecliptic plane; Complex interaction with streamer

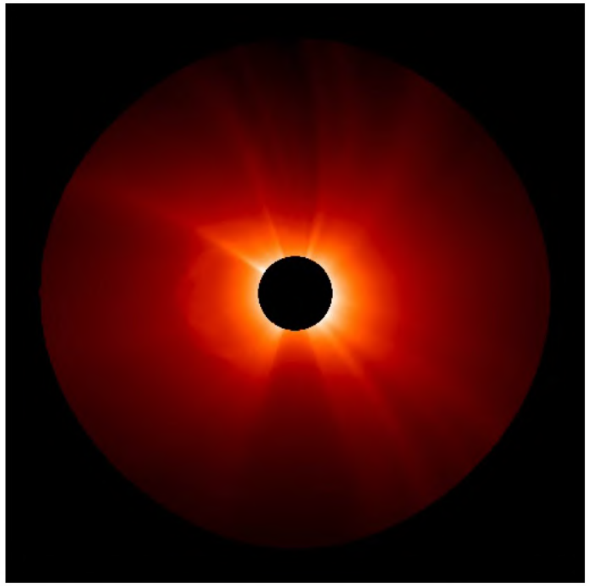

Polarized Brightness – Obs. 1

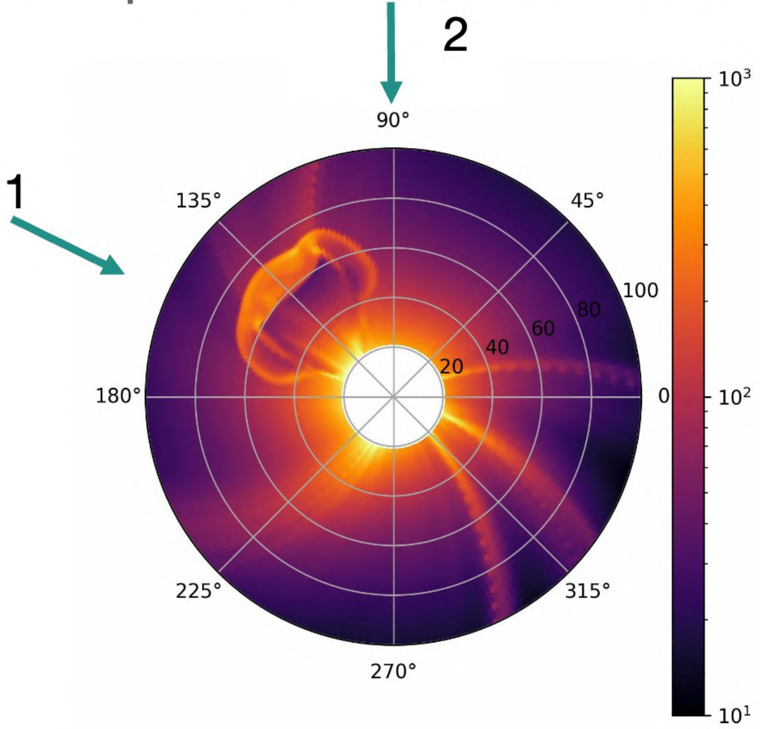

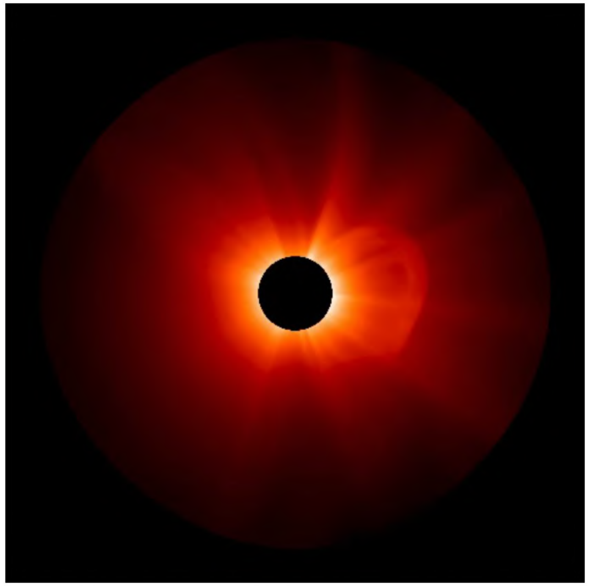

Polarized Brightness – Obs. 2

Tomographic reconstructions

Thomson Scattering

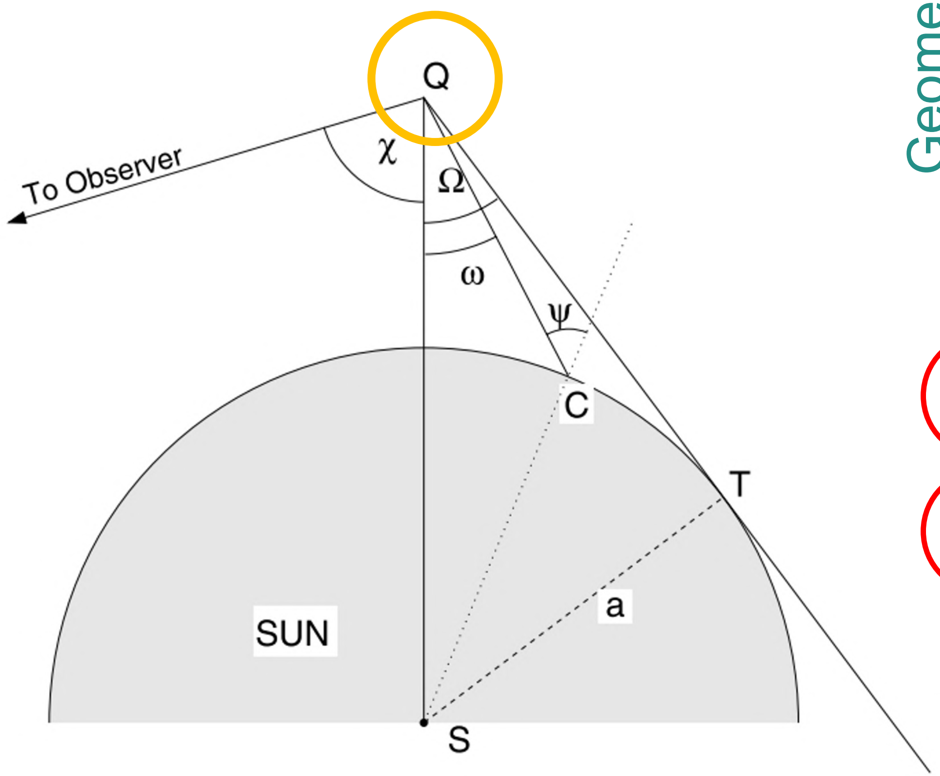

Howard, Timothy A., and S. James Tappin. "Interplanetary coronal mass ejections observed in the heliosphere: 1. Review of theory." *Space science reviews* 147 (2009): 31-54.

Geometry

$$A = \cos\Omega \sin^2\Omega,$$

$$B = -\frac{1}{8}\left[1 - 3\sin^2\Omega - \frac{\cos^2\Omega}{\sin\Omega}(1 + 3\sin^2\Omega)\ln\left(\frac{1+\sin\Omega}{\cos\Omega}\right)\right],$$

$$C = \frac{4}{3} - \cos\Omega - \frac{\cos^3\Omega}{3},$$

$$D = \frac{1}{8}\left[5 + \sin^2\Omega - \frac{\cos^2\Omega}{\sin\Omega}(5 - \sin^2\Omega)\ln\left(\frac{1+\sin\Omega}{\cos\Omega}\right)\right].$$

$$I_T = I_0 \frac{\pi\sigma_e}{2z^2}[(1-u)C + uD]$$

$$I_P = I_0 \frac{\pi\sigma_e}{2z^2}\sin^2\chi\,[(1-u)A + uB]$$

$$I_{tot} = 2I_T - I_P$$

Observed brightness depends on scattering **geometry**

Ghost trajectories can be unphysical solutions (DeForest et al. 2013)

Brightness and temporal evolution provides spatial information

Approach: **PINeRF** Physics-Informed Neural Network (PINN) + Neural Radiance Field (NeRF)

1. For each viewpoint and each pixel in the image, sample points along the line-of-sight.

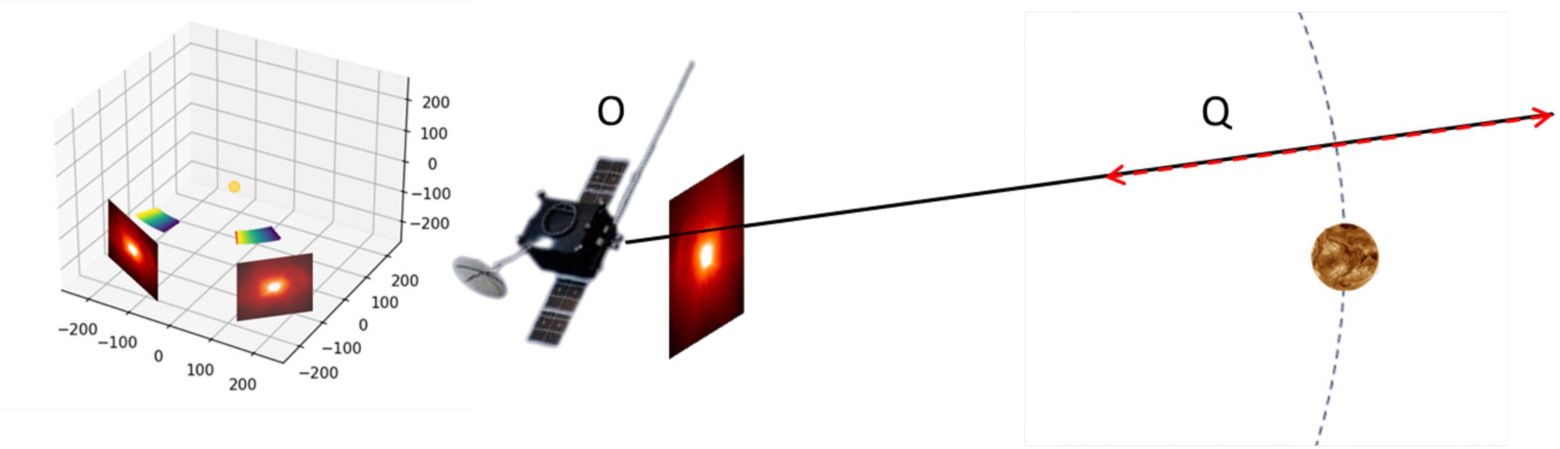

4. Establish physics constraints.

Continuity loss: $\mathcal{L}_c = \left|\frac{\partial \rho}{\partial t} + \nabla \cdot (\rho \mathbf{u})\right|$

Radial loss: $\mathcal{L}_r = \left\|\frac{\mathbf{u}}{\|\mathbf{u}\|_2} - \hat{e}_r\right\|_2$

Velocity loss: $\mathcal{L}_v = \left|\|\mathbf{u}\|_2 - \mathbf{u}_{\text{target}}\right|$

Mass only enters through the inner boundary and leaves through the outer boundary

2. Forward pass for each sampled point.

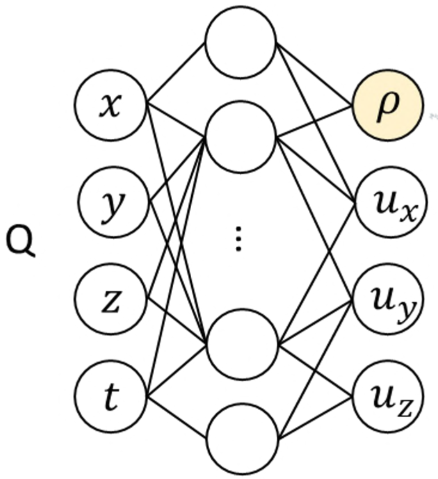

3. For each pixel, integrate the intensity from Thomson scattering to reconstruct the pixel value (prediction).

$$\tilde{I}_{\text{pixel}} = \int I_{\text{Thomson}}(O, Q)\rho(Q)dQ$$

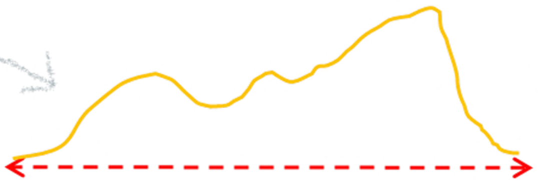

5. Optimise to match observed pixel value and physics constraints.

$$\mathcal{L}_{\text{total}} = \left|\tilde{I}_{\text{pixel}} - I_{\text{pixel}}\right| + \lambda_c \mathcal{L}_c + \lambda_r \mathcal{L}_r + \lambda_v \mathcal{L}_v$$

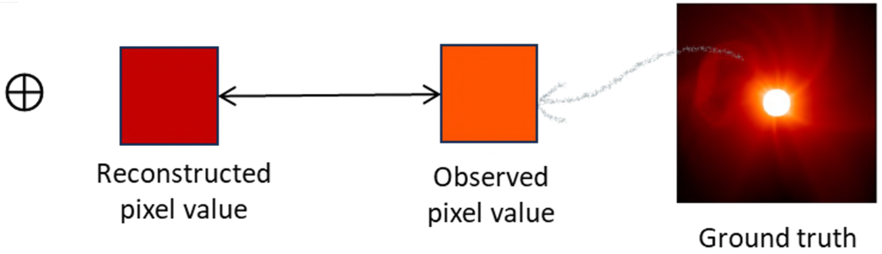

Combining multi-viewpoint observations

Reconstruction based on **6 ecliptic viewpoints (60° separation)**

Modeled observations of reconstruction:

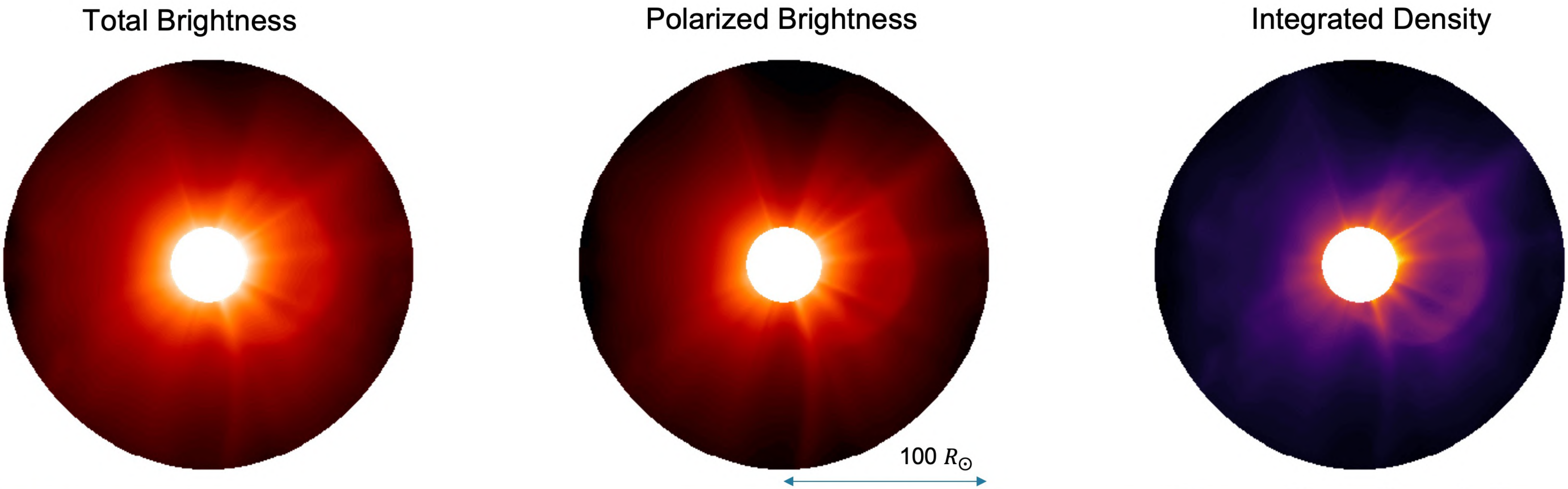

Limited number of viewpoints

Comparison of electron density in the ecliptic slice (21.5 – 100 $R_\odot$)

CME eruption at 0° Latitude

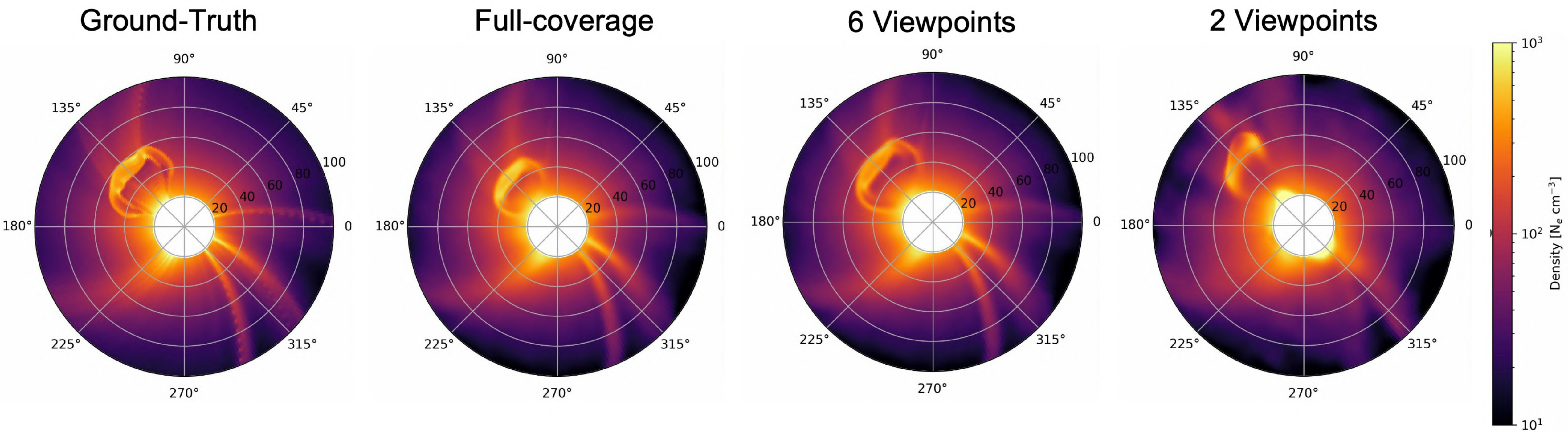

Limited number of viewpoints – 2 observers

6 Viewpoints

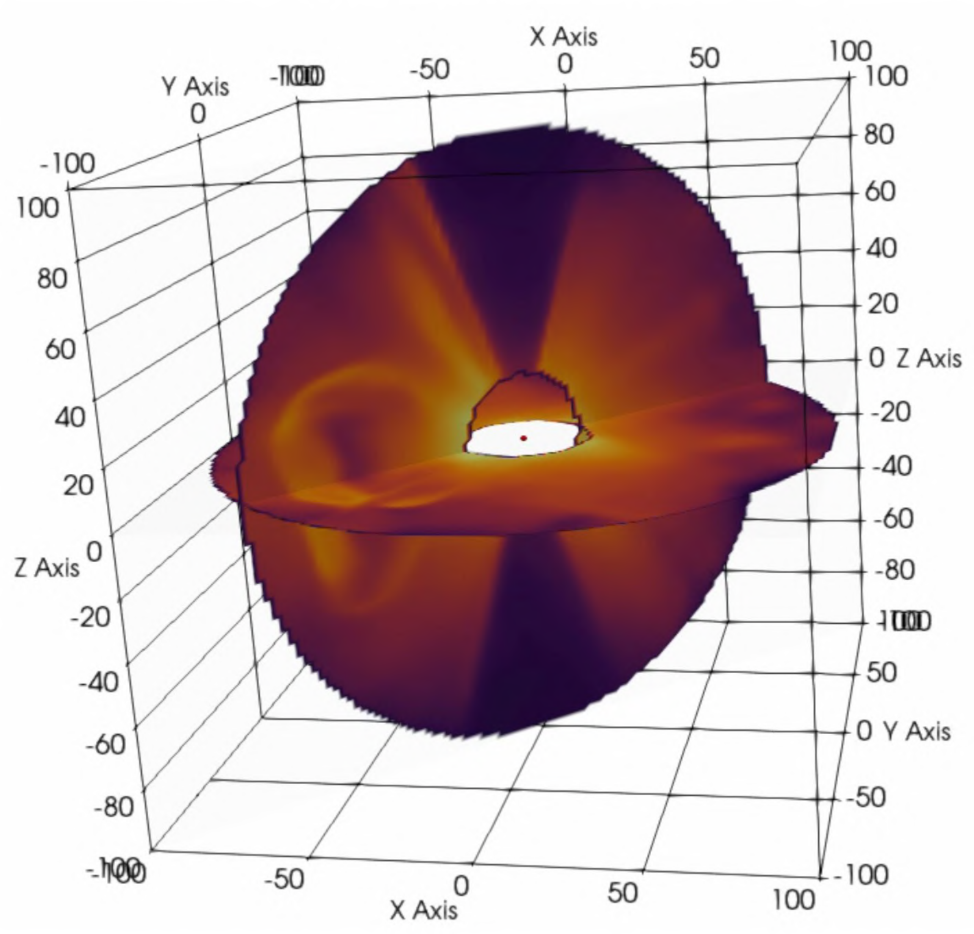

2 Viewpoints

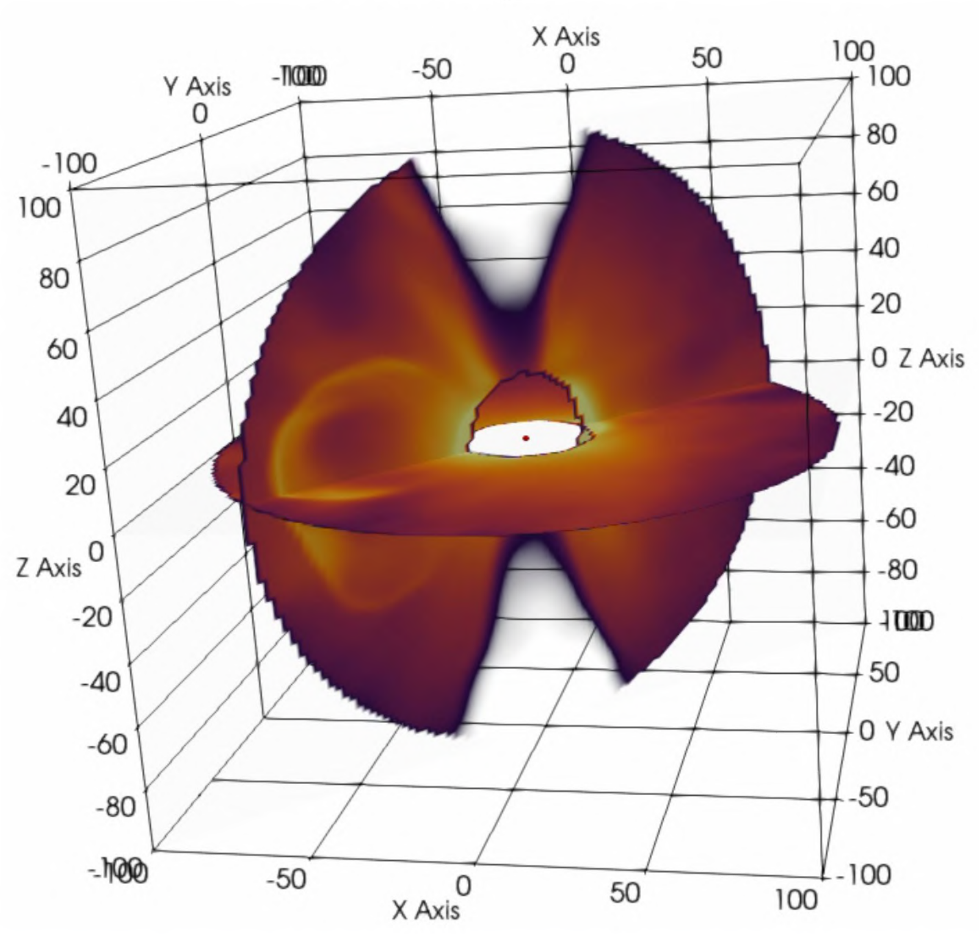

Viewpoint dependency

- Electron density reconstruction based on viewpoint
- 2 observers
  (60° separation; green arrows)
- Ecliptic slice (21.5 – 100 $R_\odot$)

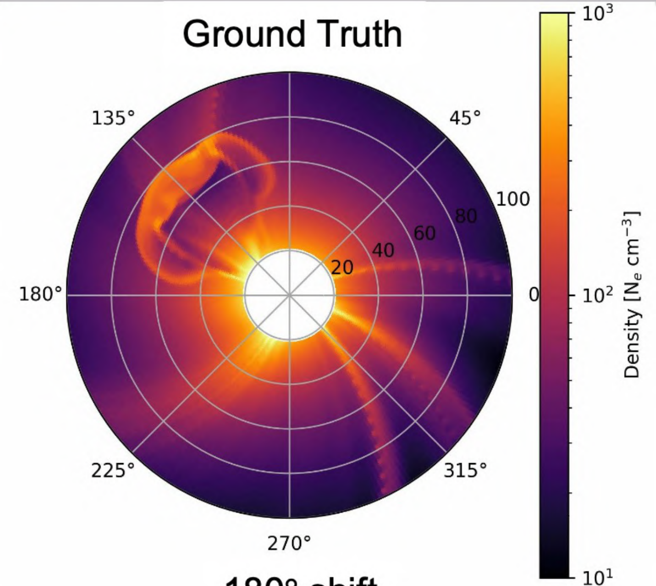

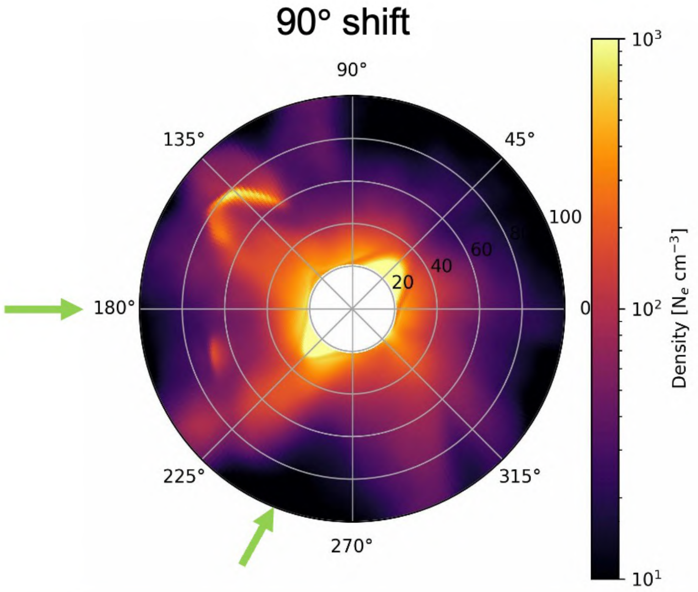

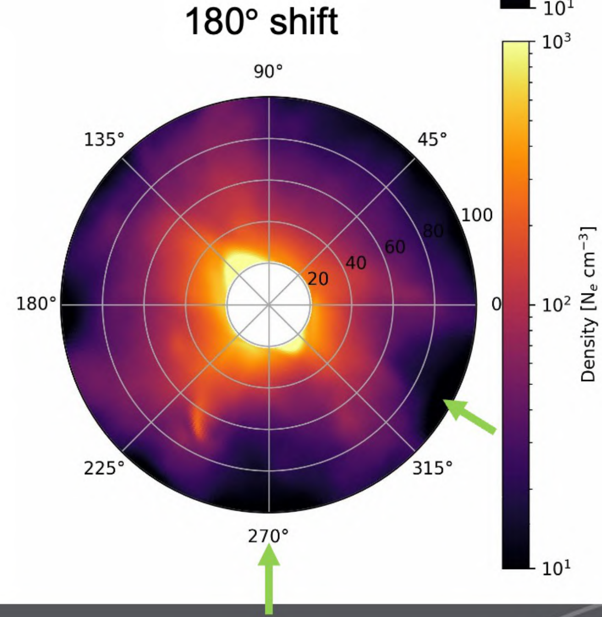

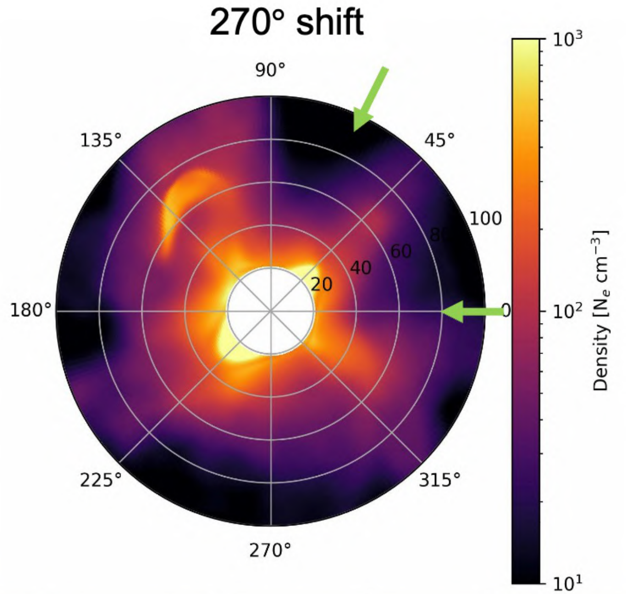

Conclusions

→ **Neural Radiance Fields enable novel tomographic reconstructions of the solar corona (EUV + white-light)**

→ **Including physical models into ray-tracing methods can overcome viewpoint limitations**

→ **Next steps:**

-Application to observations

(STEREO, SOHO; → PUNCH, VIGIL)

-Connecting domains and physics

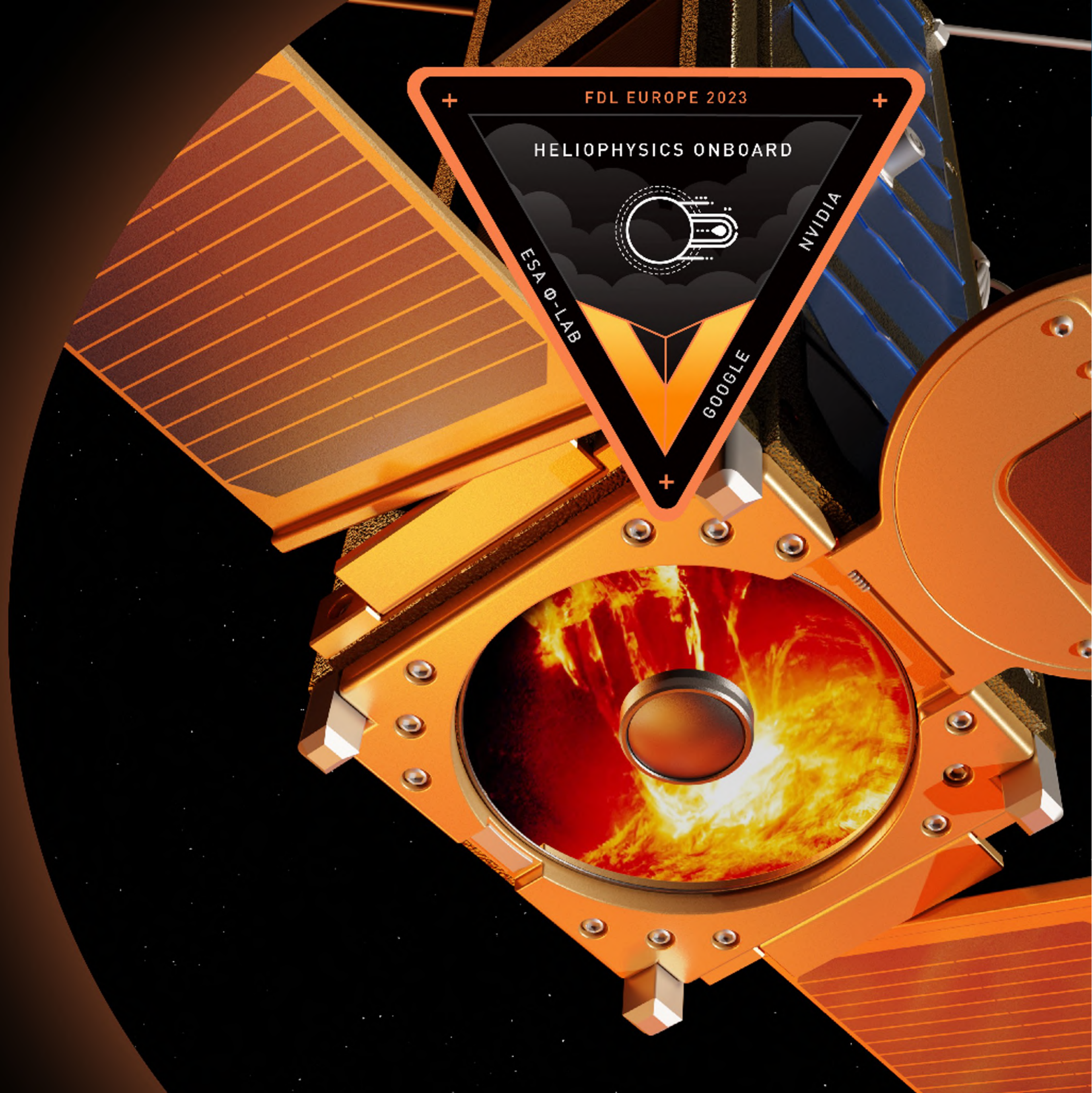

References

- Raissi, M., Perdikaris, P. & Karniadakis, G. E. Physics-informed neural networks: A deep learning framework for solving forward and inverse problems involving nonlinear partial differential equations.Journal of Computational Physics 378, 686–707 (2019).
- Karniadakis, George Em, et al. "Physics-informed machine learning." Nature Reviews Physics 3.6 (2021): 422-440.
- Bintsi, Kyriaki-Margarita, et al. "SuNeRF: Validation of a 3D Global Reconstruction of the Solar Corona Using Simulated EUV Images." arXiv preprint arXiv:2211.14879 (2022).
- Jarolim, Robert, et al. "SuNeRF: 3D reconstruction of the solar EUV corona using Neural Radiance Fields." The Astrophysical Journal Letters 961.2 (2024): L31.
- Verbeke, Christine, M. Leila Mays, Christina Kay, Pete Riley, Erika Palmerio, Mateja Dumbović, Marilena Mierla et al. "Quantifying errors in 3D CME parameters derived from synthetic data using white-light reconstruction techniques." Advances in space research (2022).
- DeForest, C. E., T. A. Howard, and S. J. Tappin. "The Thomson Surface. II. Polarization." The Astrophysical Journal 765, no. 1 (2013): 44.

Backup Slides

3D reconstruction of the EUV corona

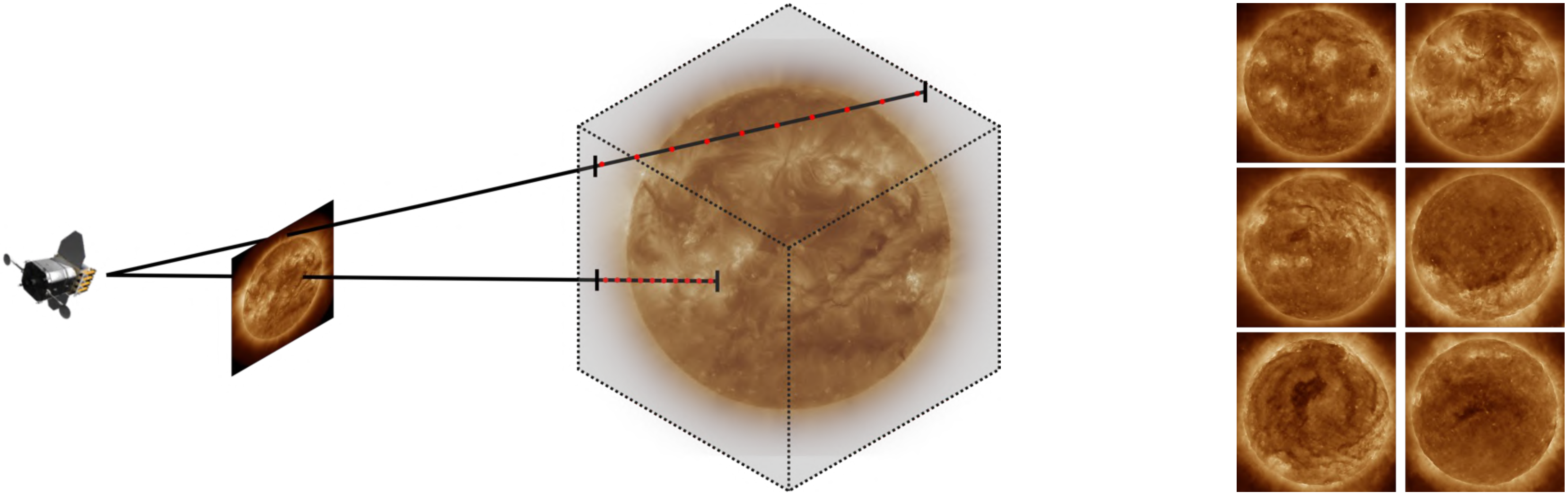

Multi-viewpoint satellite data → 3D + temporal representation (SuNeRFs) → Novel perspectives

Application to Filament Eruption

Reconstruction from 2 viewpoints (SDO/AIA + STEREO-A/EUVI)
3D reconstruction of filament eruption

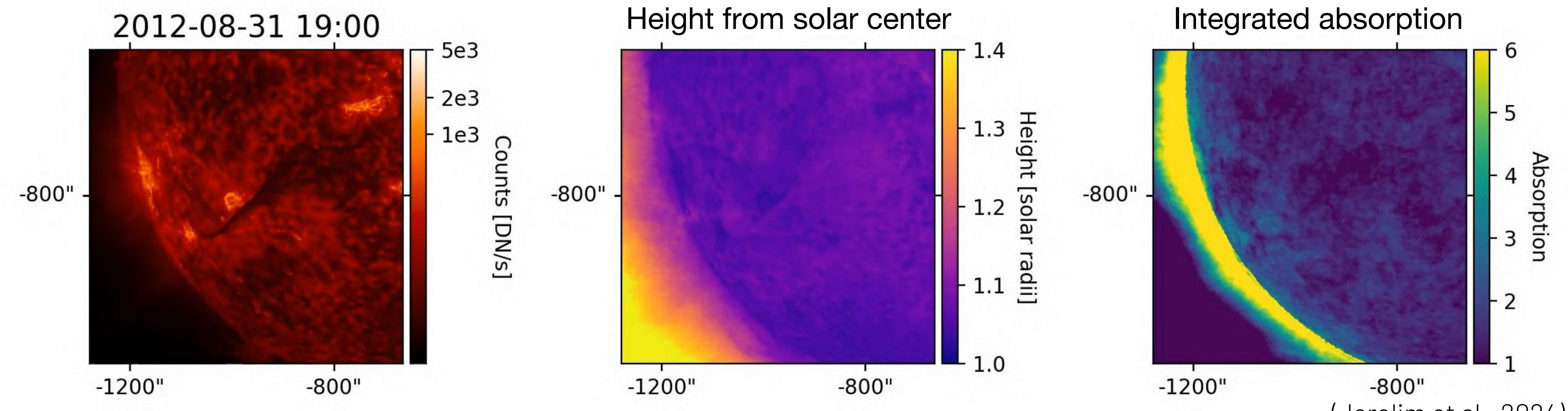

(Jarolim et al., 2024)

Application to Filament Eruption

Reconstruction from 2 viewpoints (SDO/AIA + STEREO-A/EUVI)
3D reconstruction of filament eruption

(Jarolim et al., 2024)